Epigenetic regulation of the tumor suppressor gene *TCF21* on 6q23-q24 in lung and head and neck cancer

Laura T. Smith*, Mauting Lin*, Romulo M. Brena*, James C. Lang†, David E. Schuller†, Gregory A. Otterson‡, Carl D. Morrison§, Dominic J. Smiraglia¶, and Christoph Plass*‖

*Division of Human Cancer Genetics, Department of Molecular Virology, Immunology and Medical Genetics, †Department of Otolaryngology, ‡Division of Hematology/Oncology, Department of Internal Medicine, and §Department of Pathology and Comprehensive Cancer Center, Ohio State University, Columbus, OH 43210; and ¶Department of Cancer Genetics, Roswell Park Cancer Institute, Buffalo, NY 14250

Communicated by Albert de la Chapelle, Ohio State University, Columbus, OH, November 28, 2005 (received for review August 22, 2005)

The identification of tumor suppressor genes has classically depended on their localization within recurrent regions of loss of heterozygosity. According to Knudson's two-hit hypothesis, the remaining allele is lost, either genetically or, more recently identified, through epigenetic events. To date, retrospective analyses have determined promoter methylation as a common alternative alteration in cancer cells to silence cancer-related genes. Here we report an application of restriction landmark genomic scanning that allows for DNA methylation profiling along a region of recurrent loss of heterozygosity at chromosome 6q23-q24. This approach resulted in the identification of a tumor suppressor gene, *TCF21*, which is frequently lost in human malignancies. We demonstrate that *TCF21* is expressed in normal lung airway epithelial cells and aberrantly methylated and silenced in the majority of head and neck squamous cell carcinomas and non-small-cell lung cancers analyzed. *TCF21* is known to regulate mesenchymal cell transition into epithelial cells, a property that has been shown to be deficient in carcinomas. We further demonstrate that exogenous expression of *TCF21* in cells that have silenced the endogenous *TCF21* locus resulted in a reduction of tumor properties *in vitro* and *in vivo*.

DNA methylation | epigenetics | 6q loss | restriction landmark genomic scanning | TCF21/POD1/Epicardin

Common chromosomal imbalances, resulting in loss of heterozygosity (LOH), have served as indicators for the presence of important tumor-associated genes localized within portions of the genome. Approaches aimed at detecting the tumor-related genes within regions of LOH have proven difficult because of the large number of potential candidate genes (1). The identification of cancer-related genes has been driven largely by the assumptions made in Knudson's "two-hit" hypothesis proposing biallelic gene inactivation (2). Mapping tumor suppressor genes within regions of allelic loss was followed by the identification of genetic mutations along the remaining allele (2). Aberrant DNA methylation in the regulatory region of cancer-associated genes has now been established as an alternative mechanism to heritably silence gene transcription (3, 4).

Based on the premise that retrospective analyses of known tumor suppressor genes are frequently methylated, our laboratory, as well as other groups, have established that tumor suppressor genes can be instead prospectively identified (5–11). Here we demonstrate the identification of a candidate tumor suppressor gene, *TCF21*, that is recurrently targeted for aberrant DNA hypermethylation from a region of LOH along 6q23-q24 in head and neck squamous cell carcinomas (HNSCC) and non-small-cell lung cancer (NSCLC) (12–15).

Results

Localization of AscI and NotI Restriction Landmark Genomic Scanning (RLGS) Fragments Within Chromosomal Region 6q23-q24. To investigate our hypothesis that aberrant promoter methylation may help pinpoint the location of a candidate tumor suppressor in regions of LOH, we chose a chromosomal region for which frequent LOH has been described in HNSCC and NSCLC as well as in other tumor types, but no tumor suppressor has been identified (16). LOH from the 9.6-Mb region of 6q23-q24 has been described in >20% of HNSCC and in ≈50% of NSCLC, and complete loss of the long arm of chromosome 6 is even more common (17–20). The complete 6q23-q24 sequence was obtained from the June 2002 BLAT database. *In silico* digestion with methylation-sensitive landmark restriction enzyme combinations used in RLGS (NotI–EcoRV–HinfI or AscI–EcoRV–HinfI) identified sequences migrating in RLGS gels. This region contains 49 genes or ESTs that may potentially be related to the disease phenotype. Based on our size restrictions, we identified 10 bacterial artificial chromosome (BAC) clones located within the region of LOH from 6q that were used as markers to scan the region for patterns of methylation (Fig. 1*A*). DNA isolated from the BAC clones was added into RLGS BAC mixing gels to identify the corresponding NotI or AscI fragments in the resultant RLGS profiles. Individual clones were assigned a unique address from the universal master RLGS profile. By using this approach, it was possible to identify the complete set of 10 size-matched NotI and AscI sites, representing 37% of these restriction sites residing within this chromosome 6 region.

RLGS Analysis of Patient Profiles. NotI and AscI RLGS profiles from normal and tumor tissues from 15 HNSCC and 24 NSCLC pairs were compared to determine the frequency of methylation along this chromosomal region. Methylated restriction sites are represented by a partial or complete RLGS fragment loss (Fig. 1*B*), whereas no change in RLGS fragment intensity indicates that the methylation status of the landmark enzyme site is maintained between normal and tumor tissues. DNA methylation frequencies appear to have a mosaic methylation pattern along the chromosomal fragment (Table 1, which is published as supporting information on the PNAS web site). Methylation assessed by RLGS along this 6q region ranged from 0% to 86% in NSCLC samples and from 0% to 67% in HNSCC (Fig. 1*C*). Hypermethylation events occurred frequently at the same RLGS loci, indicating that these sequences represent hot spots for aberrant DNA methylation and may be important for tumorigenesis.

Identification of a Commonly Methylated Sequence near *TCF21*. BAC clone RP11-465P13, containing AscI fragment 6E12, was lost in 86% of NSCLC ($n = 19$ of 22) and 67% of HNSCC ($n = 10$ of 15) patient profiles (Fig. 1*C*), making it the single most frequent methylation event identified in this sample set. A BLAT search of the AscI–EcoRV sequence revealed that a6E12 corresponds with a CpG island within the 5′ region of TCF21 (transcription

Conflict of interest statement: C.P. is a consultant for Epigenomics.

Abbreviations: LOH, loss of heterozygosity; RLGS, restriction landmark genomic scanning; HNSCC, head and neck squamous cell carcinoma; NSCLC, non-small-cell lung cancer; COBRA, combined bisulfite restriction analysis; BAC, bacterial artificial chromosome.

‖To whom correspondence should be addressed at: Division of Human Cancer Genetics, Ohio State University, Medical Research Facility 464A, 420 West 12th Avenue, Columbus, OH 43210. E-mail: christoph.plass@osumc.edu.

www.pnas.org/cgi/doi/10.1073/pnas.0510171102

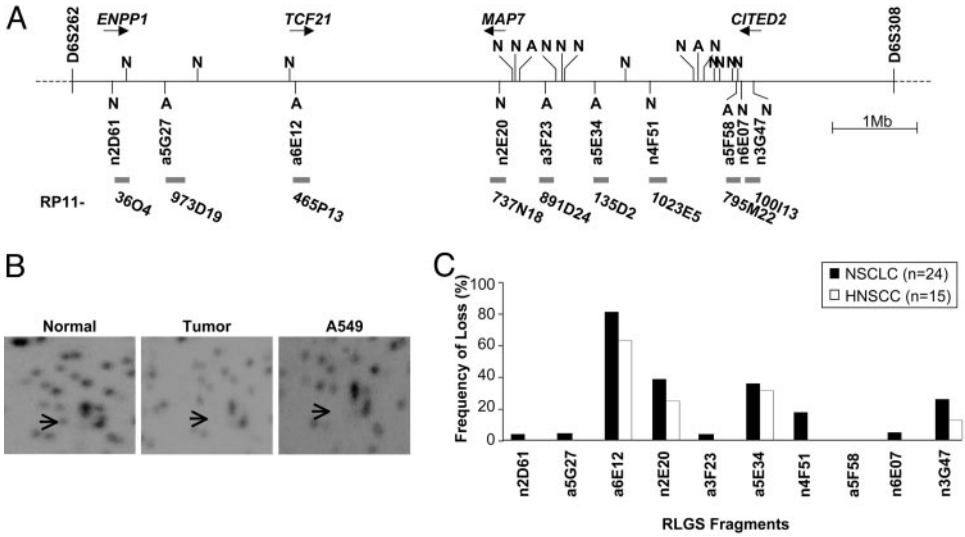

Fig. 1. 6q23-q24 DNA methylation profiling. (*A*) *In silico* digestion of the DNA sequence from 6q23-q24 identified five NotI and five AscI (N and A below the line) sites that migrate on an RLGS profile. Other NotI ($n = 15$) and AscI ($n = 2$) sites (N and A above the line) are too large or small for separation by RLGS. BACs containing the RLGS fragments are denoted with "RP11." Known genes with corresponding RLGS fragments are indicated with arrows representing orientation. (*B*) RLGS quadrant depicting unmethylated AscI fragment 6E12 (arrow) in NSCLC patient 5 normal that is methylated in the paired tumor and A549 cell line. (*C*) Methylation percentages for each clone are denoted for NSCLC (black bars) and HNSCC (white bars).

control factor 21; GenBank accession no. AF047419). The position of the AscI site is within a CpG island that spans part of exon 1 from base pair +193 after the transcriptional start site to 493 bp into intron 1.

***TCF21* Hypermethylation in Neoplastic Cells.** To determine the extent of aberrant DNA methylation in patient samples, bisulfite sequencing of six pairs of normal and tumor samples (three HNSCC sets and three NSCLC sets), as well as from a cell line derived from either HNSCC and NSCLC, was performed by using bis1, bis2, and bis3 primer pairs that encompass the CpG island (Fig. 5*A*, which is published as supporting information on the PNAS web site). Bis1, bis2, and bis3 PCR products contain 19, 19, and 15 potentially methylated CpG sites, respectively. Bisulfite sequencing of HNSCC patient 8, 54, and 56 normal and tumor cells, HNSCC cell line SCC11B, NSCLC patient 6, 11, and 16 normal and tumor cells, and NSCLC cell line H2086 revealed statistically significant differences between *TCF21* methylation in neoplastic and nonneoplastic samples in bis1, bis2, and bis3 regions ($P < 0.0085$, $P < 0.0082$, and $P < 0.0004$, respectively) (Fig. 5 *B* and *C*).

In addition to tumor-specific methylation of *TCF21* as identified by RLGS and bisulfite sequencing, methylation analysis in a larger patient population was performed to measure the extent of epigenetic regulation. A collection of bisulfite-treated DNAs from 21 HNSCC tumor and normal pairs were subject to quantitative combined bisulfite restriction analysis (COBRA). The 292-bp PCR product of *TCF21* bis1 contains three BstUI sites (Fig. 6, which is published as supporting information on the PNAS web site). The percentage of DNA methylation was obtained by relating the samples with a standard curve generated by *in vitro* methylated control samples.

COBRA analysis confirmed a higher degree of DNA methylation in the tumor samples than in their normal tissue controls overall (Fig. 2*A*). In many tumors, the banding patterns represent complete methylation (Fig. 6). Normal adjacent tissues were largely unmethylated overall, but some partial methylation represented by the 216/218-bp fragment was observed, indicating that this BstUI site is normally partially methylated.

Hypermethylation of *TCF21* Results in Gene Silencing. RNA was isolated from the patient samples used for COBRA analysis to correlate the amount of *TCF21* mRNA and DNA methylation in primary samples. Overall tumor samples with higher levels of CpG island hypermethylation had decreased *TCF21* expression (Fig. 2*B*). We observed reduced levels of *TCF21* in 16 of the 21 tumors as compared with their individual normal controls. Of these 16, 81% ($n = 13$) had higher levels of *TCF21* DNA hypermethylation than matched normal tissue, as expected. Three samples had reduced expression without hypermethylation, possibly because of other inactivating mechanisms, such as somatic mutations or LOH. Two samples that had higher DNA methylation in the tumor showed increased expression. Increased *TCF21* expression in these samples may reflect that DNA methylation of the CpG island does not alone cause transcriptional repression. Other modulators of expression, including histone modifications and alterations to transcription factors or repressors, may be required for gene expression.

Although the known expression of *TCF21* has been reported in mesenchymal cells, we wanted to confirm that *TCF21* was expressed in cells that could give rise to carcinomas, namely epithelial cells. We confirmed nuclear staining of TCF21 in normal airway epithe-

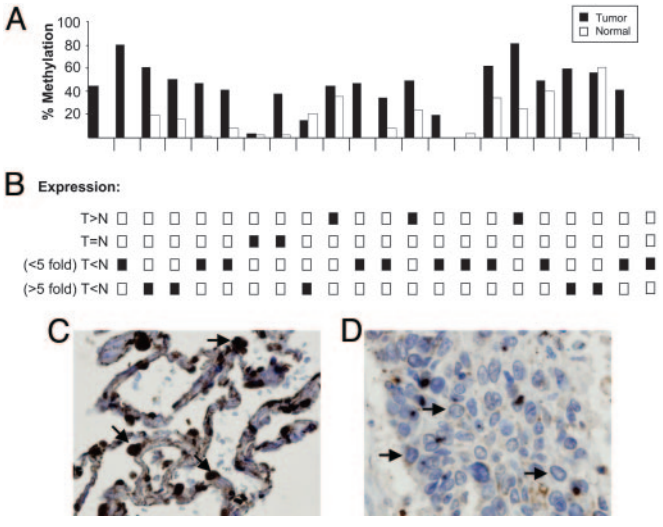

Fig. 2. COBRA and expression. (*A*) DNA methylation in paired normal and tumor samples by COBRA digestion by using BstUI in the bis1 PCR product. (*B*) Semiquantitative RT-PCR analysis of *TCF21* on the samples assessed for DNA methylation by COBRA. Expression patterns were divided into categories of tumor equal to normal (T=N), less expression in tumor compared with normal (T<N) at either <5-fold or >5-fold, and tumor expression greater than normal (T>N). (*C* and *D*) Immunohistochemical staining by using an antibody against TCF21 on normal alveolar epithelium (*C*) demonstrating nuclear expression (arrows) and a non-small-cell carcinoma section (*D*) under ×40 magnification.

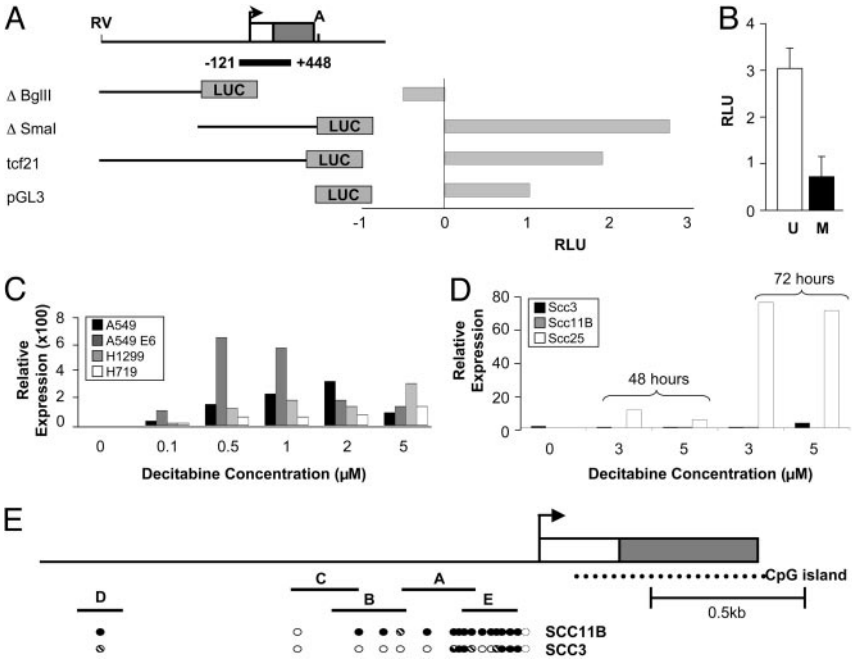

Fig. 3. Determining the promoter of *TCF21*. (*A*) TCF21-pGL3 luciferase constructs. (*B*) Luciferase activity of the tcf21 construct upon *in vitro* methylation (black bar) or no methylation (white bar). (*C* and *D*) Relative expression of *TCF21* after decitabine treatment (*x* axis) in lung cancer cell lines A549, A549E6, H719, and H1299 (*C*) and HNSCC cell lines SCC3, SCC11B, and SCC25 (*D*). (*E*) Direct sequencing of bisulfite PCR products A–E in SCC11B and SCC3. Methylation status of cytosine is shown as follows: filled circle, methylated; open circle, unmethylated; hashed circle, partial.

lium ($n = 9$) by immunohistochemistry (Fig. 2*C*). TCF21 was expressed strongly in alveolar epithelium and weakly in bronchiolar epithelium (data not shown). In addition, we stained sections prepared from NSCLC ($n = 10$) and found no nuclear TCF21 staining (Fig. 2*D*). Therefore, we were able to demonstrate that TCF21 is present in adult epithelial cells of the lung, whereas silencing occurs in cancer epithelium.

We next sought to determine the effects of DNA methylation within the *TCF21* promoter. Promoter prediction programs (http://rulai.cshl.org/tools/FirstEF) have identified an ≈600-bp region from 121 bp upstream of the transcription start site stretching 448 bp into exon 1. To determine which region contains promoter activity, portions upstream of the transcription start site, as well as the CpG island portion of *TCF21*, were examined for promoter activity *in vitro* using a luciferase reporter assay (Fig. 3*A*). The constructs containing the predicted promoter region demonstrate the highest levels of luciferase activity. The BglII construct, which does not contain the promoter portion, lacks transcriptional activity and may harbor sequences that negatively regulate *TCF21* transcription.

Based on these studies, an additional experiment to determine a direct consequence of DNA methylation within the 5′ regulatory region of *TCF21* was performed by using the "tcf21" construct (Fig. 3*A*) because it contains not only the predicted promoter region but also the CpG island portion of *TCF21* where we have identified aberrant methylation in tumors. *In vitro*-methylated sequences of the *TCF21* promoter were ligated to unmethylated pGL3. Methylating this portion of *TCF21* resulted in a >75% reduction in promoter activity (Fig. 3*B*), supporting our observation that DNA methylation regulates *TCF21* expression.

We further tested the effects of DNA methylation on gene expression *in vitro* using varying dosages of decitabine in cancer cell lines, where *TCF21* is methylated and silenced. Decitabine treatment of A549, A549 E6, H1299, and H719 lung cancer cell lines and HNSCC cell lines SCC11B and SCC25 resulted in *TCF21* gene reactivation (Fig. 3 *C* and *D*). However, as a control, in SCC3, where *TCF21* is expressed in the untreated population, decitabine had little effect. This finding indicates that *TCF21* expression is regulated by DNA methylation, whether directly through demethylation within the *TCF21* regulatory region or through reexpression of an upstream activator. To further confirm this result we performed bisulfite sequencing in SCC3 and SCC11B along the bis1, bis2, and bis3 sequences of the CpG island to determine whether aberrant DNA methylation correlates with *TCF21* silencing. Surprisingly, although it was heavily methylated, we did not see differences in DNA methylation along the CpG island region between SCC3 and SCC11B, indicating that this region may not be responsible for direct silencing.

Therefore, we used these cell lines for bisulfite sequencing of the upstream region of *TCF21*, from approximately −2 kb to −0.1 kb upstream of the transcription start site, containing 17 of 20 possible CpG sites (Fig. 3*E*). By direct sequencing of the PCR product, we identified a region from −1 kb to −0.1 kb (in products A, B, and E; see Fig. 3*E*) that show differences in DNA methylation between expressing and nonexpressing cell lines. Differences in DNA methylation in regions A and B may also account for primary samples analyzed by COBRA in Fig. 2 that do not follow the expected pattern of methylation and TCF21 transcriptional silencing; however, these experiments have not been done.

***TCF21* Overturns Neoplastic Properties.** The lung cancer cell line A549 was shown by RLGS to have a hypermethylated AscI site in the CpG island of *TCF21*. Furthermore, A549 lacks endogenous *TCF21* expression; therefore, transfection studies were performed in this cell line through a retroviral construct of pBABE-mycTCF21 to understand *TCF21*'s role in cellular control. *In vitro* comparison of individual growth rates in *TCF21*-expressing versus nonexpressing cells was performed. Overexpression of *TCF21* in A549 resulted in a reduction in the growth rate of the cells ($P < 0.0007$), without visible cell death. Cells infected with the empty vector were able to grow more than twice as rapidly as *TCF21*-expressing lines (Fig. 4*A*).

Another hallmark of a cancer cell is the loss of contact inhibition. Thus, *TCF21*-expressing and nonexpressing A549 cells were further analyzed for growth differences through colony-formation assays. Nonexpressing cells were able to establish more than seven times the number of colonies as were cells expressing *TCF21* ($P < 0.0068$) (Fig. 4*B*). Together, these results indicate a significantly stunted ability for cells expressing *TCF21* to maintain their tumorigenic properties of uncontrolled cell growth and aggregation.

Neoplastic cells often lose their differentiated epithelial cell status and express markers of an undifferentiated mesenchymal

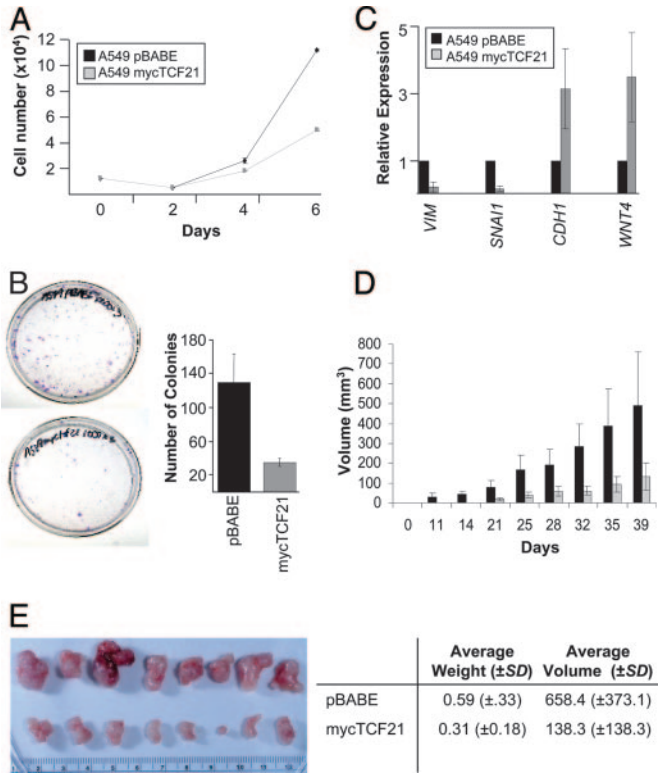

	Average Weight (±SD)	Average Volume (±SD)
pBABE	0.59 (±.33)	658.4 (±373.1)
mycTCF21	0.31 (±0.18)	138.3 (±138.3)

Fig. 4. *TCF21* reduces cancer properties. (*A* and *B*) Growth curves (*A*) and colony formation assays (*B*) on A549-pBABE and A549-mycTC21 cells. (*C*) Expression of mesenchymal markers (*VIM* and *SNAI1*) and epithelial markers (*CDH1* and *WNT4A*) in A549-pBABE and A549-mycTCF21 cells. (*D*) *In vivo* determination of tumor differences. (*E Left*) *Ex vivo* imaging of tumors isolated 40 days after injection. A549-pBABE tumors are in the top row, and A549-mycTCF21 tumors are in the bottom row. *Ex vivo* volumes and weights are summarized in *E Right*.

cell, indicating their increased ability for migration and independence from surrounding cell structures. *TCF21* functions to induce mesenchymal-to-epithelial transitions during embryogenesis, so it is possible that its exogenous expression *in vitro* induces differentiation as well. Markers such as *VIM* and *SNAI1* are expressed in mesenchymal cells, and *CDH1* and *WNT4* are expressed in epithelial cells. Gene expression patterns, as assessed through semiquantitative RT-PCR in A549-pBABE and A549-mycTCF21, were investigated for *VIM*, *SNAI1*, *CDH1*, and *WNT4*. As expected, A549-pBABE cells express five times the amount of *VIM* and seven times more *SNAI1* than the cell lines expressing *TCF21*. Expression of both *CDH1* and *WNT4* were 3-fold higher in *TCF21*-positive cells (Fig. 4*C*).

Based on *in vitro* results, we decided to pursue the relationship of *TCF21* expression and tumor growth *in vivo*. A549-pBABE cells were injected into the left dorsal side of nude mice, and A549-mycTCF21 cells were injected into the right sides. After a 5-week period for tumor growth, statistically significant differences in the two populations were visibly and measurably observed ($P = 0.0097$). Tumors that developed on the pBABE side were much larger than those that formed from the *TCF21*-positive population, with a 10-day earlier onset (Fig. 4*D*). At the conclusion of the experiment, the mice were killed and the tumors were surgically removed (Fig. 4*E*). Upon removal, weights and volumes were determined for each tumor. The tumors lacking *TCF21* expression were two to three times larger than *TCF21*-positive tumors, obtaining statistically significant different weights ($P < 0.025$). Of note, the tumors that lack *TCF21* were also more vascular, possibly indicating that angiogenesis is affected by *TCF21* expression.

Discussion

In this study we combine genetic and epigenetic information to identify a candidate tumor suppressor, *TCF21*, through a modification of the RLGS tool, in order to identify methylation at specific chromosomal regions. These data translate into a DNA methylation map that provides information regarding genes along 6q23-q24. We found that CpG island methylation along 6q23-q24 was not uniformly distributed, suggesting that there may be intrinsic sequence differences or that methylation at certain loci provides a growth advantage promoting clonal outgrowth of cells harboring this particular altered DNA methylation signature.

Our results demonstrate that *TCF21* promoter hypermethylation occurs at greater rates than somatic mutations and reported incidences of LOH along chromosome 6q (17, 19, 20). *TCF21* expression in the A549 lung cancer cell line significantly reduced tumor properties as compared with A549 cells lacking *TCF21 in vitro* and *in vivo*. Of note, the location of *TCF21* is 19 Mbp proximal to the investigated lung cancer susceptibility locus, which peaks at 6q25.2, and thus is most likely not the lung cancer susceptibility gene (18). It is also possible that other genes localized within this region could possess tumor suppressor function, but their epigenetic inactivation is not included based on assay restrictions. However, recurrent hypermethylation of *TCF21* specifically in tumor tissue across different anatomical locations and patients, and a significant reduction in growth potential of cancer cells upon *TCF21* expression, support our hypothesis that *TCF21* is a previously unidentified tumor suppressor gene that is frequently silenced by hypermethylation in cancer.

TCF21 encodes a basic helix–loop–helix transcription factor that is expressed in the mesenchyme encapsulating the epithelia of internal organs during embryogenesis and is expressed in specific tissues of the adult (22, 23). Basic helix–loop–helix proteins are transcriptional regulators that mandate cell fate differentiation (24, 25). *TCF21* is the first transcription factor identified as being essential for differentiation of epithelial cells adjacent to mesenchyme, but it joins the list of transcription factors already identified as aberrantly hypermethylated in cancer (24). Tcf21$^{-/-}$ mice are viable but have difficulties in respiration and die within minutes of birth because of poor lung differentiation (24). Perinatal lethality is a classic feature of tumor suppressor activity (26). Lung branching is a highly regulated process that is required to allow for increased surface area for gas exchange. Despite mesenchymal cell-specific expression in development, elimination of *TCF21* results in major phenotypic defects in the adjacent epithelium (23, 24, 27–30). These defects are likely because cross-talk between the supporting mesenchyme and the organ epithelium is essential for proper branching and differentiation (24, 31). However, our immunohistochemistry demonstrates epithelial-based expression of TCF21, indicating that there may be an unknown function in the adult lung. Morphologic evaluation indicates that the positively staining cells may be precursor cancer stem cells in the respiratory epithelium (32).

Loss of the TCF21 transcription factor results in a failure of mesenchymal epithelialization, a process known as mesenchymal-to-epithelial transition. Epithelial-to-mesenchymal transition (EMT) is a normal process by which a differentiated epithelial cell acquires characteristics that allow for dedifferentiation into a mobile mesenchymal cell (27, 33). The majority of human malignancies are derived from cells of epithelial origin and are termed carcinomas. Dynamic transitioning between epithelial cell to mesenchymal cell is proposed as fluctuating during tumorigenesis (35). EMT has been described in many cancers, including oral squamous cell carcinomas (36), and correlates with clinical outcome. In general, less differentiated tumors are more aggressive (37, 38). Malignant lesions are often defined by their differentiation status, where benign tumors typically retain their epithelial phenotype and malignant cells acquire a more fibroblastic mesenchymal phenotype (34). Along the invasive front of a carcinoma, epithelial cells often

gain mesenchymal cell characteristics and gene expression profiles (39). Our data demonstrate that *TCF21* results in reduced *SNAI1* and *VIM* expression as well as up-regulation of *CDH1*, a marker of organized epithelial cells (33). This finding indicates that *TCF21* has induced differentiation *in vitro*, possibly through mesenchymal–epithelial transitions, a process largely controlled by changes in transcription factor expression (34).

Interestingly, loss of chromosome 6q16-q24, including the *TCF21* locus, has been associated with metastatis (12, 40–42). To invade surrounding tissue and spread to additional sites, tumor epithelial cells adopt migration mechanisms found in normal processes (34, 35, 43). Epithelial cells obtain genetic and epigenetic modifications through epithelial-to-mesenchymal transition that permit invasion along the basement membrane, establishing an opportunity for metastasis. Once in the blood or lymphatic circulation, cells reach target organs and may be able to reestablish themselves as new lesions. Propagation of these secondary lesions is maintained by restructuring their gene expression patterns from migratory (mesenchymal) to stationary (epithelial) through mesenchymal-to-epithelial transition (35). We propose that *TCF21* is regulated primarily by DNA hypermethylation rather than genetic mutations in cancer. Commitment to inactivation by means of permanent genetic mutations does not allow flexibility in gene expression required for these changes in expression profile or the flexibility in differentiation states. DNA methylation, although a covalent modification, can be reversed, and expression of the silenced target can be restored, translating into cellular plasticity. Together, our data suggest that *TCF21* is a tumor suppressor gene from 6q23-q24 that is silenced by DNA methylation.

Materials and Methods

Tissue Collection. Frozen normal adjacent tissue and tumor tissues from HNSCC and NSCLC patients were obtained from Ohio State University through the Cooperative Human Tissue Network. All sample collection was performed in accordance with National Institutes of Health guidelines and was performed under a protocol approved by Ohio State University's Institutional Review Board. Histopathological evaluation was performed on all samples to confirm the predominance of neoplastic cells.

Identification of NotI and AscI Clones. The 6q23-q24 genomic DNA sequence was downloaded from the June 2002 BLAT resource web site (http://genome.ucsc.edu). An *in silico* digestion identified potential RLGS fragments and their corresponding first- and second-dimension sequences from the NotI–HinfI–EcoRV or AscI–HinfI–EcoRV fragments. Because of separation constraints, NotI–EcoRV or AscI–EcoRV fragments >0.7 kb and <5 kb as well as containing a NotI–HinfI or AscI–HinfI fragment size >0.12 kb were used for our analysis. BAC clones containing these fragments were ordered through the BACPAC Resource Center at Children's Hospital Oakland Research Institute (Oakland, CA) from the RPCI-11 human BAC library, isolated by Maxi-Prep (Qiagen, Valencia, CA), and confirmed by end-sequencing.

RLGS. RLGS was performed on normal adjacent and primary HNSCC and NSCLC tissue samples according to a published protocol (21). For RLGS BAC mixing gels, 0.5 ng of radiolabeled BAC DNA was mixed with labeled genomic DNA. Enhanced fragments were assigned addresses from the RLGS master profile (44). RLGS profiles from HNSCC and NSCLC were analyzed for methylation differences by comparing patients' normal and tumor profiles for 6q23-q24 loci. Methylation was classified by either a partial or a complete loss of RLGS fragment intensity.

Bisulfite Sequencing. DNA samples from were modified with sodium bisulfite treatment as described in ref. 8. *TCF21* bis1–3 and A–E bisulfite sequencing primers were designed to span the 5′ end of the gene (see Table 2, which is published as supporting information on the PNAS web site). PCR products were purified by using the gel extraction kit (Qiagen). Purified PCR products were cloned into the TOPO-TA vector (Invitrogen) by using the manufacturer's standard protocol. Five to 10 clones were sequenced from each sample.

COBRA. *In vitro* methylated DNA, representing 100% methylated DNA, and unmodified peripheral blood lymphocytes from the same individual, representing 0% methylated DNA, were combined in various ratios to create standard controls. Two micrograms of DNA was treated with sodium bisulfite overnight. Bisulfite DNA was amplified by using the *TCF21* bis1 primers. PCR products were purified by the gel extraction kit by using a modified 5-min spin after the addition of QG and PE buffers (Qiagen) to remove residual salt and ethanol from the membrane. The samples were eluted in 30 μl of TE buffer. Fifteen microliters was digested in a total volume of 30 μl containing 5 units of BstUI (NEB), 1× BSA, and 1× buffer 2 at 60°C for 3 h. Fifteen microliters of each digest was visualized on an 8% polyacrylamide gel, and the remaining digest was quantitated (Agilent, Palo Alto, CA) (see *Supporting Methods*, which is published as supporting information on the PNAS web site).

Decitabine Treatment. NSCLC cell lines (A549, A549 E6, H719, and H1299) were plated in 10-cm^2 culture dishes in triplicate. Cell cultures were treated with 0.1–1 μM decitabine (5-aza-2′-deoxycytidine, Sigma) for 48 h. SCC3, SCC11B, and SCC25 HNSCC cell lines were treated with 3 and 5 μM decitabine for 48 and 72 h. Media-containing drug was replaced every 24 h to avoid drug hydrolysis and inactivation. Control plates were treated with equal amounts of dimethyl sulfoxide. After treatment, the cells were grown in regular culture media for an additional 24 h.

Semiquantitative RT-PCR. RNA was isolated by using TRIzol (Invitrogen). cDNA was synthesized from 2 μg of total RNA by using the SuperScript first-strand synthesis kit (Invitrogen) oligo(dT) and random hexamers in a 2.5-μl reaction. Semiquantitative RT-PCRs were carried out by using the IQ SYBR green Supermix (Bio-Rad). For detailed information, see *Supporting Methods.*

Immunohistochemistry. Histological sections (4 μM) were obtained from tumor tissue ($n = 10$) and normal adjacent tissue ($n = 9$) from patients with NSCLC. A primary antibody derived from an epitope directed against human TCF21 was commercially available (sc-15007, Santa Cruz Biotechnology). Slides were incubated with a 1:25 dilution of the primary antibody.

Construction of the *TCF21* Promoter Plasmids. The *TCF21* promoter sequence (from base pairs −1320 to +688) was amplified by PCR using primers tagged with KpnI and XhoI restriction site cloned into TOPO-TA (Invitrogen), and subsequently, cloned into pGL3 to create pGL3-tcf21. Deletion constructs along the upstream portion of *TCF21* were derived from this plasmid by using the restriction sites indicated in Fig. 4*A*. All clones were sequence-verified.

Methylated *TCF21* Promoter Luciferase Constructs. Twenty micrograms of the pGL3-TCF21 was digested with 40 units of XhoI (NEB) followed by 20 units of KpnI. pGL3 vector and TCF21 insert bands were extracted from a 0.8% agarose gel by using the gel extraction kit. Insert DNA was eluted in 50 μl of buffer elution buffer and separated into two fractions, whereas the pGL3 vector remained free of additional modifications. Twenty microliters of insert DNA was incubated for 2 h at 37°C with methyl donor, *S*-adenosylmethionine, and in the presence or absence of SssI (30 units). DNA was purified by using the gel extraction kit and eluted in 30 μl of elution buffer. Completeness of the *in vitro* methylation reactions was determined through methylation-sensitive and -in-

sensitive restriction enzyme digestion with HpaII and MspI, respectively. Methylated and unmethylated inserts were ligated into pGL3. The ligation product was phenol chloroform/isoamyl alcohol purified and used for transfection. Luciferase activity was normalized by cotransfection of *Renilla*-TK.

***TCF21* Retroviral Vector.** The *TCF21* ORF containing mRNA sequence from +248 to +921 was cloned into TOPO-TA in the multiple cloning site. The 200-bp myc tag (8) was PCR-amplified by using primers containing a KpnI restriction site at the end of the forward primer and a SpeI restriction site at the end of the reverse primer, and directionally cloned into TOPO-TA upstream of TCF21 ORF. The mycTCF21 insert was PCR-amplified from this plasmid by using primers that recognize the 5′ portion of the myc tag and contain a BamHI site and a TCF21 reverse primer containing a 3′ SalI site, ligated to pBABE, and transformed into Top10 cells (Invitrogen). Plasmid DNAs were sequence-confirmed.

Transfection. Ten micrograms of pBABE-mycTCF21 plasmid or pBABE vector alone was transfected into the amphotropic Phoenix packaging cell line (60% confluent) by using SuperFect (Qiagen). Viral medium was collected, and cell debris was removed by centrifugation. Four milliliters of infectious medium was added to the surface of 40% confluent A549 cells. After 12 h, the infectious medium was replaced, and the infection was repeated. Selection medium containing 5 μg/ml puromycin (Sigma) was added to the cell cultures the following day. Whole-protein lysate was isolated and tested for the presence of mycTCF21 by Western blot with a MYC-specific primary antibody (Cell Signaling Technology, Beverly, MA).

Growth Curves. Cell-cycle synchronization was performed by culturing cells in the absence of FBS for 12 h. A total of 1×10^4 cells were plated twice in triplicates for 2, 4, and 6 days in selection medium. Cells were then counted in duplicate with the Coulter Z particle counter (Coulter, Fullerton, CA) and averaged.

Colony Formation. A total of 1×10^3 cells were plated in triplicate in selection medium for 14 days. Cells were washed once with PBS and fixed in methanol:acetic acid (3:1) twice for 5 min and once for 15 min, then stained with 0.1% crystal violet in PBS for 30 min at room temperature.

Nude Mouse Injections. A total of 1.5×10^6 A549-mycTC21 cells were injected s.c. into the right rear flanks of eight athymic nude mice (The Jackson Laboratory), and A549-pBABE cells were injected into the left rear flanks of the same mice as a control. Tumor volumes were determined twice weekly by caliper measurement. The calculated radius was then used to determine the tumor volume. Tumors were extracted and measured 5 weeks after injection.

Statistical Evaluations. Statistical analyses provided were all based on the paired *t* test.

We thank Ramana Davuluri and Sandya Liyanarachchi for help with statistical evaluation, members of the C.P. laboratory for critical evaluation of the manuscript, and Thomas E. Carey (University of Michigan, Ann Arbor) for contributing HNSCC cell lines. This work was supported in part by National Institutes of Health Training Grant CA009338 and National Institute of Dental and Craniofacial Research Grant DE13123 (to C.P.).

1. Tomlinson, I. P., Lambros, M. B. & Roylance, R. R. (2002) *Genes Chromosomes Cancer* **34,** 349–353.
2. Knudson, A. G. (2001) *Nat. Rev. Cancer* **1,** 157–162.
3. Baylin, S. B., Esteller, M., Rountree, M. R., Bachman, K. E., Schuebel, K. & Herman, J. G. (2001) *Hum. Mol. Genet.* **10,** 687–692.
4. Herman, J. G. & Baylin, S. B. (2003) *N. Engl. J. Med.* **349,** 2042–2054.
5. Jones, P. A. & Baylin, S. B. (2002) *Nat. Rev. Genet* **3,** 415–428.
6. Tran, T. N., Liu, Y., Takagi, M., Yamaguchi, A. & Fujii, H. (2005) *J. Oral Pathol. Med.* **34,** 150–156.
7. Zardo, G., Tiirikainen, M. I., Hong, C., Misra, A., Feuerstein, B. G., Volik, S., Collins, C. C., Lamborn, K. R., Bollen, A., Pinkel, D., *et al*. (2002) *Nat. Genet.* **32,** 453–458.
8. Dai, Z., Popkie, A. P., Zhu, W. G., Timmers, C. D., Raval, A., Tannehill-Gregg, S., Morrison, C. D., Auer, H., Kratzke, R. A., Niehans, G., *et al*. (2004) *Oncogene* **23,** 3521–3529.
9. Pfeifer, G. P., Yoon, J. H., Liu, L., Tommasi, S., Wilczynski, S. P. & Dammann, R. (2002) *Biol. Chem.* **383,** 907–914.
10. Tomizawa, Y., Sekido, Y., Kondo, M., Gao, B., Yokota, J., Roche, J., Drabkin, H., Lerman, M. I., Gazdar, A. F. & Minna, J. D. (2001) *Proc. Natl. Acad. Sci. USA* **98,** 13954–13959.
11. Dammann, R., Li, C., Yoon, J. H., Chin, P. L., Bates, S. & Pfeifer, G. P. (2000) *Nat. Genet.* **25,** 315–319.
12. Barghorn, A., Speel, E. J., Farspour, B., Saremaslani, P., Schmid, S., Perren, A., Roth, J., Heitz, P. U. & Komminoth, P. (2001) *Am. J. Pathol.* **158,** 1903–1911.
13. Stenman, G., Sandros, J., Mark, J. & Edstrom, S. (1989) *Cancer Genet. Cytogenet.* **39,** 153–156.
14. Stenman, G., Sandros, J., Dahlenfors, R., Juberg-Ode, M. & Mark, J. (1986) *Cancer Genet. Cytogenet.* **22,** 283–293.
15. Sandros, J., Mark, J., Happonen, R. P. & Stenman, G. (1988) *Anticancer Res.* **8,** 637–643.
16. Knuutila, S., Aalto, Y., Autio, K., Bjorkqvist, A. M., El-Rifai, W., Hemmer, S., Huhta, T., Kettunen, E., Kiuru-Kuhlefelt, S., Larramendy, M. L., *et al*. (1999) *Am. J. Pathol.* **155,** 683–694.
17. Girard, L., Zochbauer-Muller, S., Virmani, A. K., Gazdar, A. F. & Minna, J. D. (2000) *Cancer Res.* **60,** 4894–4906.
18. Bailey-Wilson, J. E., Amos, C. I., Pinney, S. M., Petersen, G. M., de Andrade, M., Wiest, J. S., Fain, P., Schwartz, A. G., You, M., Franklin, W., *et al*. (2004) *Am. J. Hum Genet.* **75,** 460–474.
19. Braakhuis, B. J., Snijders, P. J., Keune, W. J., Meijer, C. J., Ruijter-Schippers, H. J., Leemans, C. R. & Brakenhoff, R. H. (2004) *J. Natl. Cancer Inst.* **96,** 998–1006.
20. Bockmuhl, U., Wolf, G., Schmidt, S., Schwendel, A., Jahnke, V., Dietel, M. & Petersen, I. (1998) *Head Neck* **20,** 145–151.
21. Okazaki, Y., Okuizumi, H., Sasaki, N., Ohsumi, T., Kuromitsu, J., Hirota, N., Muramatsu, M. & Hayashizaki, Y. (1995) *Electrophoresis* **16,** 197–202.
22. Lu, J., Richardson, J. A. & Olson, E. N. (1998) *Mech. Dev.* **73,** 23–32.
23. Lu, J. R., Bassel-Duby, R., Hawkins, A., Chang, P., Valdez, R., Wu, H., Gan, L., Shelton, J. M., Richardson, J. A. & Olson, E. N. (2002) *Science* **298,** 2378–2381.
24. Quaggin, S. E., Schwartz, L., Cui, S., Igarashi, P., Deimling, J., Post, M. & Rossant, J. (1999) *Development* **126,** 5771–5783.
25. Funato, N., Ohyama, K., Kuroda, T. & Nakamura, M. (2003) *J. Biol. Chem.* **278,** 7486–7493.
26. Meuwissen, R. & Berns, A. (2005) *Genes Dev.* **19,** 643–664.
27. Lu, J., Chang, P., Richardson, J. A., Gan, L., Weiler, H. & Olson, E. N. (2000) *Proc. Natl. Acad. Sci. USA* **97,** 9525–9530.
28. Cui, S., Ross, A., Stallings, N., Parker, K. L., Capel, B. & Quaggin, S. E. (2004) *Development* **131,** 4095–4105.
29. Bukovsky, A., Caudle, M. R., Keenan, J. A., Upadhyaya, N. B., Van Meter, S. E., Wimalasena, J. & Elder, R. F. (2001) *BMC Dev. Biol.* **1,** 11.
30. Gibson, M. C. & Perrimon, N. (2003) *Curr. Opin. Cell Biol.* **15,** 747–752.
31. Shannon, J. M. & Hyatt, B. A. (2004) *Annu. Rev. Physiol.* **66,** 625–645.
32. Kim, C. F., Jackson, E. L., Woolfenden, A. E., Lawrence, S., Babar, I., Vogel, S., Crowley, D., Bronson, R. T. & Jacks, T. (2005) *Cell* **121,** 823–835.
33. Prindull, G. & Zipori, D. (2004) *Blood* **103,** 2892–2899.
34. Kiemer, A. K., Takeuchi, K. & Quinlan, M. P. (2001) *Oncogene* **20,** 6679–6688.
35. Thiery, J. P. (2002) *Nat. Rev. Cancer* **2,** 442–454.
36. Friedl, P. & Wolf, K. (2003) *Nat. Rev. Cancer* **3,** 362–374.
37. Welch, D. R. & Rinker-Schaeffer, C. W. (1999) *J. Natl. Cancer Inst.* **91,** 1351–1353.
38. Yoshida, B. A., Sokoloff, M. M., Welch, D. R. & Rinker-Schaeffer, C. W. (2000) *J. Natl. Cancer Inst.* **92,** 1717–1730.
39. Miyazawa, J., Mitoro, A., Kawashiri, S., Chada, K. K. & Imai, K. (2004) *Cancer Res.* **64,** 2024–2029.
40. Welch, D. R., Chen, P., Miele, M. E., McGary, C. T., Bower, J. M., Stanbridge, E. J. & Weissman, B. E. (1994) *Oncogene* **9,** 255–262.
41. Miele, M. E., Jewett, M. D., Goldberg, S. F., Hyatt, D. L., Morelli, C., Gualandi, F., Rimessi, P., Hicks, D. J., Weissman, B. E., Barbanti-Brodano, G. & Welch, D. R. (2000) *Int. J. Cancer* **86,** 524–528.
42. Shirasaki, F., Takata, M., Hatta, N. & Takehara, K. (2001) *Cancer Res.* **61,** 7422–7425.
43. Boyer, B., Valles, A. M. & Edme, N. (2000) *Biochem. Pharmacol.* **60,** 1091–1099.
44. Costello, J. F., Fruhwald, M. C., Smiraglia, D. J., Rush, L. J., Robertson, G. P., Gao, X., Wright, F. A., Feramisco, J. D., Peltomaki, P., Lang, J. C., *et al*. (2000) *Nat. Genet.* **24,** 132–138.